Letter

Chinese Science Bulletin

High-Energy Physics

September 2012 Vol.57 No.27: 3556–3559
doi: 10.1007/s11434-012-5397-3

An ultralow-energy negative cluster ion beam system and its application in preparation of few-layer graphene

WANG ZeSong[1], ZHANG ZaoDi[1], ZHANG Rui[1], WANG ShiXu[1], FU DeJun[1*] & LIU JiaRui[1,2]

[1] *Key Laboratory of Artificial Micro- and Nano-Materials of Ministry of Education of China, School of Physics and Technology, Wuhan University, Wuhan 430072, China;*
[2] *Texas Center for Superconductivity, University of Houston, Houston, Texas 77004, USA*

Received April 14, 2012; accepted July 8, 2012

We developed a cluster ion beam system that produces negative cluster beams of C_1–C_{10} with ion current of 4.5 nA–50 μA at extraction voltages ranging from 6 to 20 kV. The system uses the injector of a tandetron accelerator and was established by inserting an electrostatic scanner on its ion-optical line and modifying its Faraday cup into a substrate holder. Utilization of clusters enables ultrashallow ion implantation at energies as low as 600 eV/atom without deceleration. Small carbon clusters C_2 and C_4 were implanted into Ni/SiO_2/Si substrates and following post-thermal treatment graphene was obtained. Raman spectroscopy showed characteristic 2D peaks with G-to-2D peak ratios revealing formation of 2–3 layers of graphene. The Raman data reveals clear effect of nonlinear cluster-surface interaction in ion beam synthesis of two-dimensional nanomaterials.

ultralow energy, cluster beam, negative ion, ultrashallow implantation, grapheme, Raman scattering

Citation: Wang Z S, Zhang Z D, Zhang R, et al. An ultralow-energy negative cluster ion beam system and its application in preparation of few-layer graphene. Chin Sci Bull, 2012, 57: 3556–3559, doi: 10.1007/s11434-012-5397-3

Graphene as a promising material has attracted much attention since 2004 for academic interest and technological importance [1]. It has become a potential candidate material for fast electronic device applications, owing to its unique two-dimensional honey comb lattice structure and extraordinary physical properties. Prior to device applications, controllable process for deposition of graphene has to be established. Up to date, mechanical exfoliation of highly oriented pyrolytic graphite [1], epitaxial graphitization of silicon carbide [2,3], chemical vapor deposition on single crystal transition metal such as Ru, Ni, Cu [4–6], and chemical reduction graphene oxide methods [7], have been reported. Most recently, ion implantation has been attempted to prepare graphene samples [8,9]; however, in the reported process, carbon ions at rather high energy (30 keV and 80 keV) were used, which would yield a broad depth-profile of carbon in the matrix and inevitably generate irradiation defects. To prepare good quality two-dimensional nanomaterials like graphene or topological insulator films, it is necessary to develop low- and ultralow-energy ion beam technologies.

In this work, we designed an ultralow-energy cluster ion beam system based on the cesium sputtering negative ion source of the injector of a tandetron accelerator, and extracted carbon cluster ion beams (C_1–C_{10}). As an example, the carbon cluster beams were implanted into Ni films to form graphene layers, which proves ultrashallow implantation to be a successful process.

The basic configuration of the modified injector consists mainly of a negative ion source, an electrostatic scanner and a sample carrier, as shown in Figure 1. The negative carbon cluster ion beam extracted from the ion source is analyzed by a switching magnet and scanned by an electric scanner prior to impinging on the substrate. Ni films with a thickness of 50 nm deposited on 300 nm-thick SiO_2/Si were used as substrates for the cluster ion implantation.

The ion source is a Cs sputtering type negative source

*Corresponding author (email: djfu@whu.edu.cn)

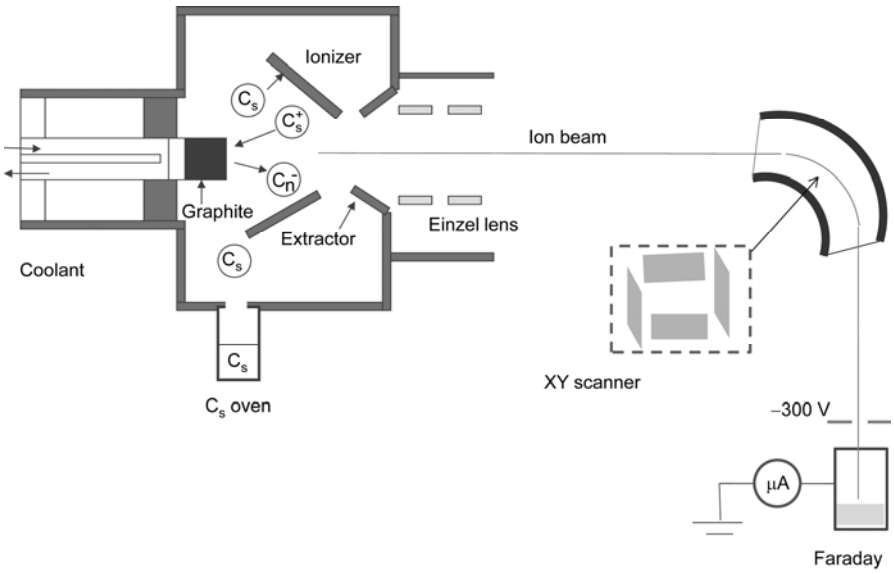

Figure 1 Schematic diagram of the negative cluster ion beam system.

consisting of a Cs reservoir, a cathode, an ionizer and an extractor. Since extraction of cluster ion beams is highly dependent on the density and morphology of the target [10], a high purity (99.999%) graphite rod was chosen for the sputtering. Cs atoms evaporated from the heated reservoir reach the high temperature region of the armored tantalum ionizer and lose their outmost electrons. The resultant Cs^+ ions are accelerated to penetrate the condensed Cs layer on the cathode and sputter the carbon atoms off the graphite target. The carbon atoms and clusters passing through the Cs layer capture electrons and become negative cluster ions. They are then accelerated to the extractor by a voltage set between 6–20 kV.

In Figure 1 the electrostatic scanner mounted between two 45° switching magnets was designed to form a 10 mm × 10 mm uniform area on the surface of the substrate, which is located 20 cm from the second magnet. The sweep voltage on the scanner is only 0–1000 V, and this novel design makes the system compact and efficient, in comparison with a previous layout [11]. C_1–C_{10} cluster beams were transported by an extraction voltage of 20 kV to the substrate where ion currents of 30–50 μA were recorded (Figure 2(a)). This means that multiplayer graphene growth needs only a few seconds of implantation. The mass spectra in Figure 2(b) and (c) show 8–10 times reduction of the current at 10 kV compared with Figure 2(a), and a further decrease at 6 kV where a few nA C_5 clusters are recorded. This is still usable since a single atomic layer needs only a few 10^{15} cm^{-2}. For a substrate tilted 30°–45° from the beam line, implantation with C_5 at 6 kV means an energy as low as 600 eV/atom, corresponding to a depth shallower than 3 nm.

As an example of the application of the cluster beams and for simplicity, we implanted Ni films by C_2 and C_4 clusters extracted by a voltage 20 kV, providing energy per atom of 10 and 5 keV, respectively.

Figure 3 shows depth profiles of C in Ni films obtained by SRIM simulation [12], assuming that every atom of the C_n clusters carries an equal energy of 20 keV and simulating single atom-solid interaction rather than cluster-solid interaction. It is clearly seen that the different C_n clusters result in different C projectiles, with projected ranges between 5–25 nm.

Taking into account of the projectiles, solubility, and re-sputtering effect, the implant dose was set 8×10^{15} cm^{-2} to prepare bilayer grapheme [8,9]. After implantation, the samples were annealed at 900°C for 50 min in vacuum and cooled to 725°C (at a rate of 5–8°C/min), followed by quenching in the air.

Confocal micro-Raman spectroscopy (Renishaw RM-1000) was employed to characterize the graphene films using an Ar^+ laser with a wavelength of 514.5 nm and a power at the sample surface below 0.4 mW. Figure 4 shows the Raman spectra of samples prepared by C_2 and C_4 implantation. The G bands at 1581–1584 cm^{-1} and 2D bands at 2705–2712 cm^{-1} represent typical sp^2 structure of crystalline graphene films. The Raman shift of the G peak is lower than the single layer graphene. The D bands at 1353–1357 cm^{-1} are associated with a high density of defects or grain boundaries in the samples arising from symmetry breaking. The intensity ratios of I_G/I_D peak (proportional to the in-plane crystalline size of the graphene lattice) and I_G/I_{2D} are 9 and 2, respectively, correlated with defects and the number of graphene layers [13–15]. The results mean that the samples are of 2–3 layers of graphene without too many defects [9]. The full width at half maximum of the 2D peak is 79–80 cm^{-1}. The D peak located at 1622 cm^{-1} and D+G at 2947 cm^{-1} are disorder activated features.

The number of graphene sheets evaluated from Raman

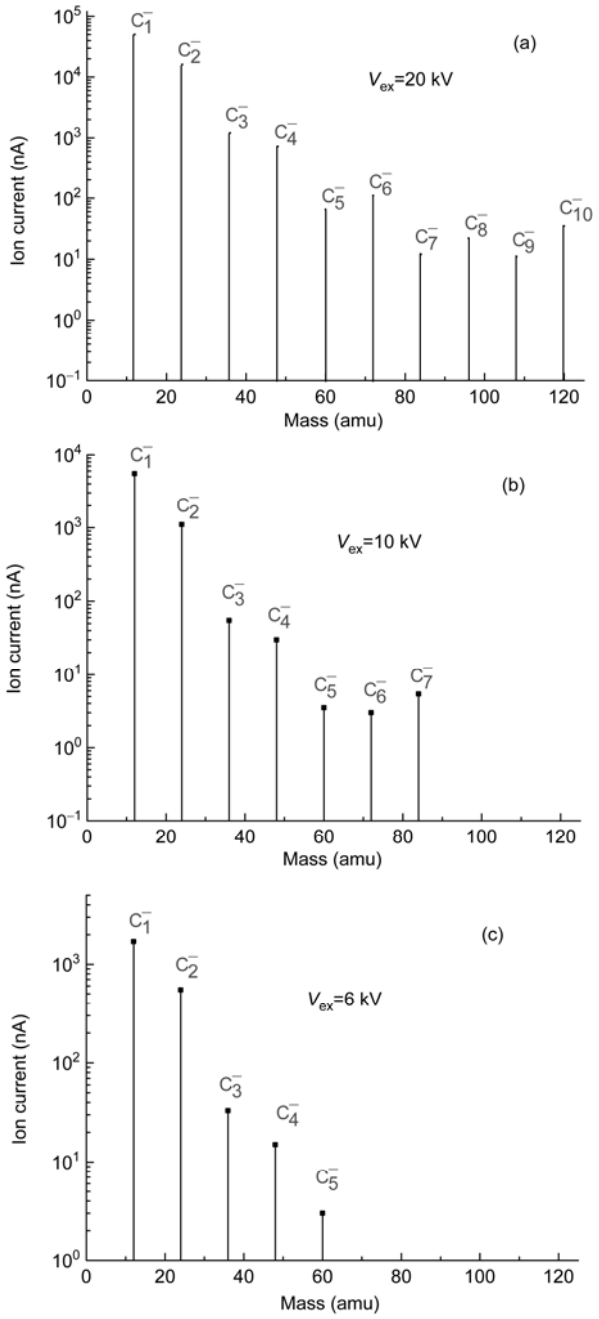

Figure 2 Mass spectra of negative carbon clusters produced by a cesium sputtering ion source at different extraction voltages (20 kV, 10 kV and 6 kV).

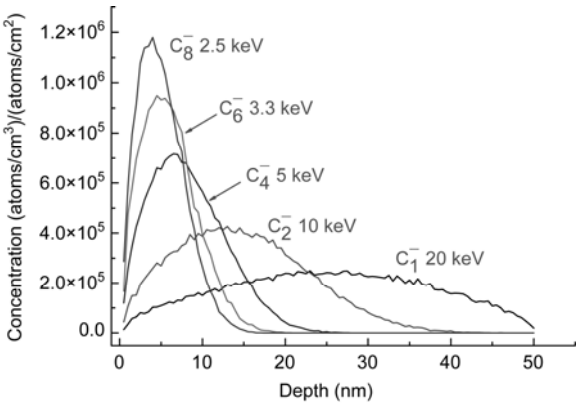

Figure 3 Depth profiles of various C_n clusters implanted in Ni films simulated by using the SRIM program.

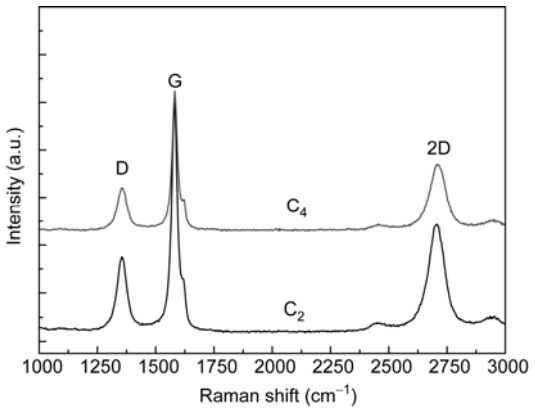

Figure 4 Raman spectra of graphene prepared by implantation of C_2 and C_4 clusters into Ni/SiO_2/Si and annealed at 900°C for 50 min followed by quenching from 725°C.

scattering is larger than expected, because the implant dose of 8×10^{15} cm^{-2} corresponds to a double graphene density that should produce bilayer graphene on the Ni surface [8,9]. This difference means that the implantation and damaging process is governed by cluster-surface interaction and cannot be taken as simple linear superposition of individual ion-solid interaction process. In fact, the implantation damage increases nonlinearly with the number of atoms of a cluster [16]. During annealing at 700°C the damages were recovered and the Ni film re-crystallized, creating nucleation points and C atoms diffused out to the Ni surface from the bulk within a few seconds [17]. Carbon atoms segregated from the Ni film due to supersaturation during annealing and subsequent quenching, and diffused to the nucleation points, forming nanocrystalline graphene (Figure 3) [15,18].

Figure 5 shows the Raman spectra of graphene prepared by C_2 and C_4 implantation annealed following a different procedure, i.e. annealing at 900°C for 50 min, and cool naturally to room temperature in the furnace ambient. The very broad D and G peaks and high intensity ratio I_D/I_G indicate that more defects were induced in Ni films during this heat treatment. The I_G/I_{2D} peak ratio is almost the same as that in Figure 4, which shows stable multilayer graphene. At the same time, the D and G+D bands have grown dramatically, reaffirming generation of more serious disorder. The comparison shows that the annealing followed by quenching process is superior to the latter. For clarity, the peak positions and intensity ratios are summarized in Table 1, which shows that the process with larger clusters involves more evident nonlinear cluster-surface interaction effect.

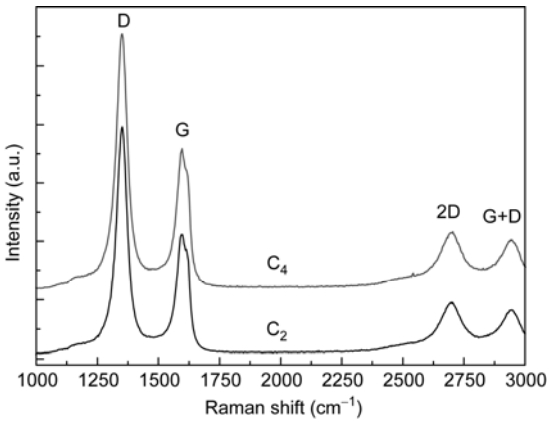

Figure 5 Raman spectra of graphene by cluster ion implantation followed by annealing at 900°C for 50 min and natural cooling to room temperature.

Table 1 Raman peak positions and intensity ratios of graphene

Cluster used	D (cm^{-1})	G (cm^{-1})	2D (cm^{-1})	I_G/I_D	I_G/I_{2D}
C_2	1355	1581	2706	2.85	2.05
C_4	1357	1584	2712	3.0	2.03

In conclusion, we have developed a negative cluster ion beam system within the injector of a 1.7 MV tandetron and delivered 4.5 nA–50 μA analyzed C_n cluster beams to the substrate holder. The cluster beam energies were 6–20 keV making it possible to conduct ultrashallow implantation down to a few nanometers. Small C_2 and C_4 clusters were implanted into Ni films to demonstrate the feasibility of graphene synthesis by the cluster ion beam technology. The Raman spectroscopy showed characteristic 2D peaks with I_G/I_{2D} ratios verifying formation of 2–3 graphene. The effect of different post-treatment schemes shows subtle but clear deviation in the structure of the resultant materials, which provides a good example for investigation of the nonlinear cluster-solid interaction.

This work was supported by the International Cooperation Program of the Ministry of Science and Technology of China (*2010DFA02010*).

1 Novoselov K S, Geim A K, Morozov S V, et al. Science, 2004, 306: 666–669
2 Berger C, Song Z, Li X, et al. Science, 2006, 312: 1191–1196
3 Reina A, Jia X T, Ho J, et al. Nano Lett, 2009, 9: 30–35
4 Marchini S, Günther S, Wintterlin J. Phys Rev B, 2007, 76: 075429
5 Kim K S, Zhao Y, Jang H, et al. Nature, 2009, 457: 706–710
6 Li X, Cai W, An J, et al. Science, 2009, 324: 1312–1314
7 Eda G, Fanchini G, Chhowalla M. Nat Nanotech, 2008, 3: 270–274
8 Garaj S, Hubbard W, Golovchenko J A. Appl Phys Lett, 2010 97: 183103
9 Baraton L, He Z B, Lee C S, et al. Nanotechnology, 2011, 22: 085601
10 Wang X M, Lu X M, Shao L, et al. Nucl Instr Meth B, 2002, 196: 198–204
11 Zhang Z D, Wang Z S, Wang S X, et al. Chin Phys Lett, 2012, 29: 078101
12 Ziegler J F. SRIM—The Stopping and Range of Ions in Matter (2008 edition), www.srim.org
13 Ni Z H, Wang Y Y, Yu T, et al. Nano Res, 2008, 1: 273–291
14 Ferrari A C, Meyer J C, Scardaci V, et al. Phys Rev Lett, 2006, 97: 187401
15 Baraton L, He Z B, Lee C S, et al. Europ Phys Lett, 2011, 96: 46003
16 Xie Z X, Wang X M, Lu X M, et al. AIP Conf Proc, 2001, 576: 987–990
17 Lander J J, Kern H E, Beach A L. J Appl Phys, 1952, 23: 1305–1309
18 Ni Z H, Wang H M, Kasim J, et al. Nano Lett, 2007, 7: 2758–2763